On-Chip Matching Networks for Radio-Frequency Single-Electron-Transistors

W. W. Xue,* B. Davis, Feng Pan, J. Stettenheim, T. J. Gilheart, and A. J. Rimberg†
6127 Wilder Lab, Department of Physics and Astronomy, Dartmouth College Hanover, NH, 03755 USA

Z. Ji
Department of Physics and Astronomy, Rice University, Houston, TX 77005 USA

In this letter, we describe operation of a radio-frequency superconducting single electron transistor (RF-SSET) with an on-chip superconducting LC matching network consisting of a spiral inductor L and its capacitance to ground C_p. The superconducting network has a lower C_p and gives a better matching for the RF-SSET than does a commercial chip inductor. Moreover, the superconducting network has negligibly low dissipation, leading to sensitive response to changes in the RF-SSET impedance. The charge sensitivity $\delta q = 2.4\times10^{-6}\, e/\sqrt{\mathrm{Hz}}$ in the sub-gap region and energy sensitivity $\delta\varepsilon = 1.9\hbar$ indicate that the RF-SSET is operating in the vicinity of the shot noise limit.

With growing interest in quantum computation,[1,2] spin-based qubits,[3,4] the quantum properties of nanomechanical resonators,[5,6] and quantum measurement[7,8] much attention has been focused on ultra-fast charge detectors such as the radio-frequency single electron transistor (RF-SET).[9,10,11,12] In rf mode, the SET is embedded in an LC network as illustrated in Fig. 1(a) allowing a working bandwidth of tens of MHz and avoiding $1/f$ noise from amplifiers and background charges. The LC network usually consists of a commercial chip inductor L and its parasitic capacitance to ground C_p; such networks, however, have drawbacks such as losses and relatively large C_p that degrade the performance of the SET.

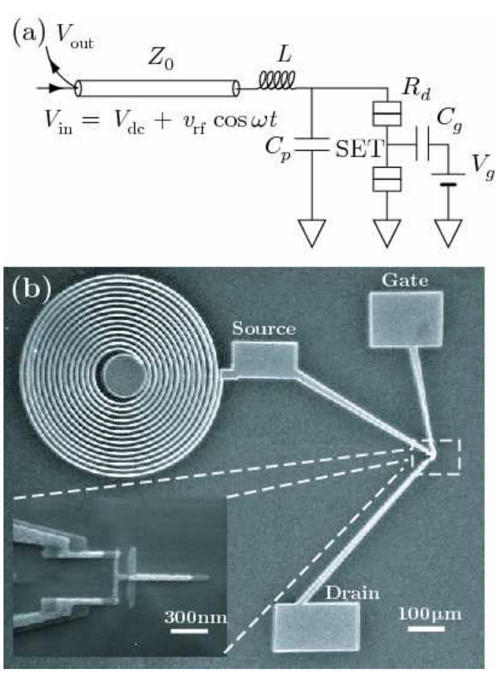

FIG. 1: (a) Idealized model of an LC matching network. (b) Optical micrograph of an on-chip matching network prior to wire bonding. The apparent inductor linewidth is set by the resolution of the image. The inset shows an electron micrograph of the SET.

In this letter, we describe RF-SSETs with on-chip fully superconducting LC matching networks. Although our best charge sensitivity $\delta q = 2.4 \times 10^{-6}\, e/\sqrt{\mathrm{Hz}}$ does not quite match the record to date[12], our SET and matching network design are not yet fully optimized. Furthermore, our measurement is in the sub-gap region for which transport occurs via a combination of Cooper pair and quasiparticle tunneling. The backaction of the SET, the rate at which it dephases a measurement,[13,14] is predicted to be smaller in the sub-gap region than in the above-gap region for which Coulomb blockade of quasiparticles dominates.[10,11,12]

Fig. 1(a) shows an idealized model for an on-chip superconducting matching network. One end of the SET is connected to an Al spiral inductor L, which is then connected via a coaxial cable to room temperature electronics. The other end of the SET is grounded directly to the cable shield. The inductor L, the SET differential resistance R_d, and the stray capacitance C_p from the inductor and SET bonding pads to ground form an LCR network with resonant frequency $f_0 \approx \frac{1}{2\pi\sqrt{LC_p}}$. A carrier wave with frequency f_0 and rms amplitude v_{rf} is applied to the network and the reflected signal is measured. The reflection coefficient at resonance is given by $\Gamma = \frac{Z_{\mathrm{in}}-50}{Z_{\mathrm{in}}+50}$ where the input impedance of the network $Z_{\mathrm{in}} = \frac{L}{R_d C_p}$. In order to optimize the charge sensitivity, Z_{in} should be impedance matched to the $50\,\Omega$ coaxial cable at the point of maximal change in SET conductance with charge. The unloaded quality factor $Q = \sqrt{\frac{L}{C_p}}\frac{1}{Z_0}$ determines the amplitude of the rf signal applied to the SET $v_{\mathrm{SET}} = 2Qv_{\mathrm{rf}}$ and the resonance bandwidth f_0/Q.

An on-chip superconducting matching network has three advantages in comparison with a commercial chip inductor. First, because C_p is smaller for an on-chip network, better impedance matching can be attained at higher frequencies, resulting in a larger resonance bandwidth for a given Q. Second, an on-chip network can be extended to multi-pole matching networks[15] that can further increase the bandwidth, possibly allowing measurements on nanosecond time scales. Finally, our on-chip LC networks are entirely superconducting at our

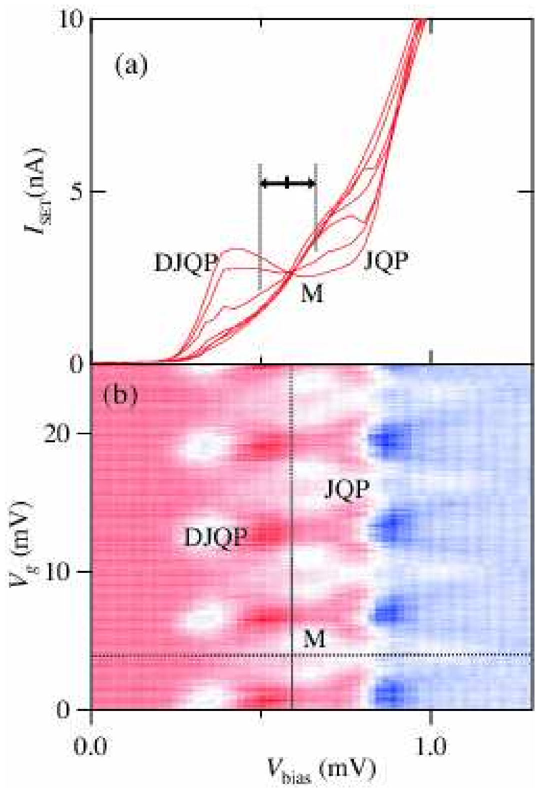

FIG. 2: (a) I-V curves of sample A for various V_g. The modulation at the DJQP and JQP features is about 2 nA. Point M shows the dc bias V_{dc} for optimal RF-SET operation and the arrows and vertical dashed lines show the peak to peak rf amplitude at the SET $v_{\mathrm{SET}} = 2Qv_{\mathrm{rf}} \approx 160\,\mu$V. (b) False-color image of G_d versus V_{dc} and V_g. Experimentally determined optimal values of V_{dc} and V_g for rf operation are indicated by the dashed lines.

measurement temperature and have negligible loss at radio frequencies. In comparison, the input impedance at resonance of a matching network that includes normal metals has loss terms arising from dissipation in the inductor L or capacitor C_p in addition to the transformed SET impedance $\frac{L}{R_d C_p}$. The reflection coefficient for a lossy network is therefore less sensitive to changes in R_d. While fully on-chip matching networks have been used previously, they have generally included some normal metal components.[6,16]

Fig. 1(b) shows an optical micrograph of an on-chip network. The network is fabricated together with the SET by e-beam lithography and double-angle shadow evaporation of Al. The number and spacing of the turns of the spiral inductor (linewidth 3μm, line spacing 20μm) determines L. The inset of Fig. 1(b) shows a scanning electron micrograph of the SET with junction area about 40×60 nm^2. The center of the spiral inductor is wire bonded using an Al wire to the central pin of a coaxial cable and the ground lead of the SET is similarly bonded to the cable shield.

The measurements were carried out in a ^{3}He refrigerator at the base temperature of 290 mK. Copper-stainless steel powder filters in the cryostat and π-type filters at room temperature were used to eliminate high frequency noise. A low-noise HEMT amplifier and directional coupler were located in the cryostat at a temperature of around 2.8 K. We made two samples with the same SET design and similar total normal-state resistance R_n: sample A was coupled to a 12-turn spiral inductor and sample B to a 14-turn inductor. DC I-V curves were measured with custom-made low noise current and voltage amplifiers, and the SET differential conductance $G_d = 1/R_d$ via standard lock-in techniques. Results for sample A are shown in Fig. 2. Features associated with two subgap charge transport cycles, the Josephson-quasiparticle (JQP) and double Josephson-quasiparticle (DJQP) cycles are clearly visible; for a detailed discussion see Ref. 17 and references therein. We determined the SET charging energy $E_c = e^2/2C_\Sigma = 205\,\mu$eV where C_Σ is the total SET capacitance from the location of the DJQP feature and $R_n = 25\,\mathrm{k}\Omega$ from the slope of the I-V curve at high bias. Similar measurements for sample B gave $E_c = 222\,\mu$eV and $R_n = 26\,\mathrm{k}\Omega$.

We found that sample B (14 turn inductor) was better matched to the coaxial line, with near perfect matching at $R_d = 20\,\mathrm{k}\Omega$. With the SET biased near the center of the gap ($R_d \gg 1\,\mathrm{M}\Omega$), virtually all the input signal is expected to be reflected. This expectation is in agreement with the data for sample B in the right inset of the Fig. 3, which shows the power P_r reflected by the tank circuit for different R_d. The top curve, which indicates P_r for $R_d \gg 1\,\mathrm{M}\Omega$, has no dip in P_r at resonance, only a background slope due to details of the rf setup. The reflection coefficient Γ shown in Fig. 3 is obtained from the data in the right inset. We assume $\Gamma = 1$ for the largest R_d and, using the top curve as a reference, calculate Γ at different R_d by taking the difference between the other curves and the reference. Virtually identical results are obtained by fitting a line to the background slope of the top curve and using the fit as the reference instead.

With decreasing R_d, Γ decreases over two orders of magnitude at resonance, reaching a minimum of $\Gamma = 0.006$ at $R_d = 19.2\,\mathrm{k}\Omega$. Our bandwidth of roughly 50 MHz $\sim f_0/Q$ is roughly three times larger than that for measurements with similar Q but lower resonant frequency.[10,11] From the ratio of Γ at resonance for any two different R_d, and the expressions for Γ, Z_{in} and f_0 given above, we calculate $Q \approx 20$, $L \approx 170$ nH and $C_p \approx 0.17$ pF for which the optimal $R_d = 20\,\mathrm{k}\Omega$. To compare with a commercial inductor, we fabricated a low-impedance sample with $R_n = 13\,\mathrm{k}\Omega$ and coupled it to the coaxial cable through a Panasonic ELJ 82 nH chip inductor. P_r for this sample, for which $f_0 = 975$ MHz and the optimal $R_d = 11\,\mathrm{k}\Omega$, is shown in the left inset of Fig. 3. We estimate $C_p \approx 0.34$ pF; the relatively large value of C_p prevents matching to larger R_d. Furthermore, a dip in P_r of about 11 dB appears at resonance for very large R_d, indicating that only about 8% of the input power is reflected. The other 92% is lost to dissipative processes

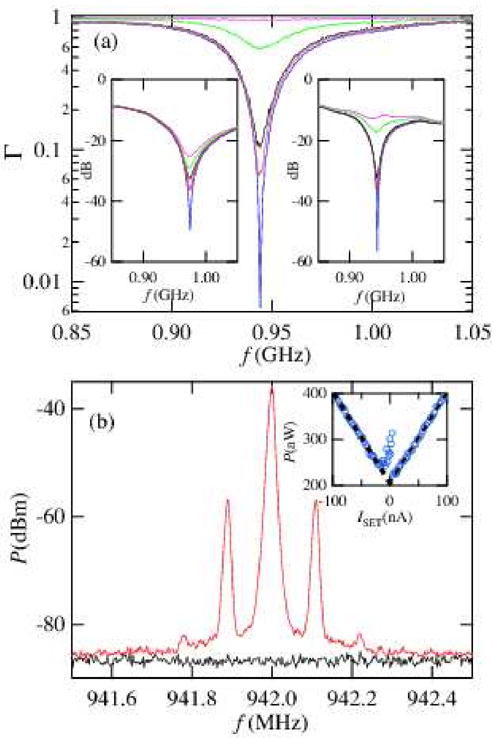

FIG. 3: (a) Γ versus frequency for sample B for different R_d as determined from lockin measurements of G_d. Top to bottom: center of the gap (pink), $R_d = 40\,\mathrm{k\Omega}$ (green), $28.2\,\mathrm{k\Omega}$ (black), $22.2\,\mathrm{k\Omega}$ (red), $19.2\,\mathrm{k\Omega}$ (blue). The inset shows reflected power P_r versus frequency for the low impedance SET and Panasonic chip inductor (left) and for sample B (right). Left inset, top to bottom: center of the gap (pink), $R_d = 37\,\mathrm{k\Omega}$ (green), $21\,\mathrm{k\Omega}$ (black), $17.8\,\mathrm{k\Omega}$ (red), $12\,\mathrm{k\Omega}$ (blue). Right inset, top to bottom: center of the gap (pink), $R_d = 40\,\mathrm{k\Omega}$ (green), $28.2\,\mathrm{k\Omega}$ (black), $22.2\,\mathrm{k\Omega}$ (red), $19.2\,\mathrm{k\Omega}$ (blue). (b) Power spectrum of the RF-SSET output for a 110 kHz $0.01e$ rms excitation. The lower line is the noise floor with no rf signal applied on the SET. Inset: total system noise at f_0 versus the dc SET current in the absence of applied rf power.

in the matching network.[18]

Response of our RF-SSETs to a charge excitation was measured with a spectrum analyzer; typical data are shown in Fig. 3(b). The charge sensitivity δq is determined from the rms charge excitation amplitude q_0 and the signal-to-noise ratio in dB (SNR) of a sideband from $\delta q = (q_0/\sqrt{2\,\mathrm{BW}})10^{-\mathrm{SNR}/20}$ where BW is the measurement bandwidth. The best charge sensitivity for sample B is $\delta q = 2.4\times10^{-6}e/\sqrt{\mathrm{Hz}}$, about three times better than that achieved with a lossy LC network and the same rf setup.[17] We calibrated our system noise temperature for sample B by measuring the total noise power versus the dc SET current I (Fig. 3(b), inset). At higher bias, the noise varies linearly with I due to the SET shot noise.[11] The contribution from the HEMT amplifier is determined by the crossing point of the two fitting curves at $I = 0$. We obtain an amplifier noise power $P_n = 210$ aW for a measurement bandwidth BW = 3 MHz, giving a noise temperature $T_n = \frac{P_n}{\mathrm{BW}k_B} = 5.3\,\mathrm{K}$. The uncoupled energy sensitivity of sample B is $\delta\varepsilon = \frac{(\delta q)^2}{2C_{\mathrm{SET}}} = 1.9\hbar$, approaching the shot noise limit for the RF-SET.[8,19] Without the contribution from the cryogenic amplifier we estimate $\delta\varepsilon = 1.2\hbar$. For sample A, we measured similar values of $\delta q = 3.1\times10^{-6}e/\sqrt{Hz}$ and $\delta\varepsilon = 3.1\hbar$.

Embedding the RF-SSET in the on-chip matching network shows potential for studying the shot noise of the SET for either rf or dc biases by making several improvements in our system. First, the R_d for optimal charge sensitivity in sample B was about 35 kΩ (point M in Fig. 2(a)), while near-perfect matching occurred at $R_d = 20\,\mathrm{k\Omega}$. Further improvements in the matching network design should allow us to reduce C_p and increase L for better matching with higher R_d without lowering the resonant frequency. Also, using a HEMT amplifier with lower noise temperature will improve both the charge and uncoupled energy sensitivity. Finally, improved fabrication techniques for the SET may also lead to a better charge sensitivity.

This work was supported by the NSF under Grant No. DMR-0454914 and by the ARO under Agreement No. W911NF-06-1-0312.

---

* Electronic address: weiwei.xue@dartmouth.edu
† Electronic address: ajrimberg@dartmouth.edu

1 P. W. Shor, in *Proceedings of the 35th Annual Symposium on the Foundations of Computer Science*, edited by S. Goldwasser (IEEE Computer Society, Los Alamitos, CA, 1994), pp. 124–134.

2 L. K. Grover, Phys. Rev. Lett. **79**, 325 (1997).

3 J. M. Elzerman, R. Hanson, L. H. Willems van Beveren, B. Witkamp, L. M. K. Vandersypen, and L. P. Kouwenhoven, Nature **430**, 431 (2004).

4 J. R. Petta, A. C. Johnson, J. M. Taylor, E. A. Laird, A. Yacoby, M. D. Lukin, C. M. Marcus, M. P. Hanson, and A. C. Gossard, Science **309**, 2180 (2005).

5 R. G. Knobel and A. N. Cleland, Nature **424**, 291 (2003).

6 M. D. LaHaye, O. Buu, B. Camarota, and K. C. Schwab, Science **304**, 74 (2004).

7 V. B. Braginsky and F. Ya. Khalili, *Quantum Measurement* (Cambridge University Press, Cambridge, 1992).

8 M. H. Devoret and R. J. Schoelkopf, Nature **406**, 1039 (2000).

9 R. J. Schoelkopf, P. Wahlgren, A. A. Kozhevnikov, P. Delsing, and D. E. Prober, Science **280**, 1238 (1998).

10 A. Aassime, G. Johansson, G. Wendin, R. J. Schoelkopf, and P. Delsing, Phys. Rev. Lett. **86**, 3376 (2001).

11 A. Aassime, D. Gunnarsson, K. Bladh, P. Delsing, and R. Schoelkopf, Appl. Phys. Lett. **79**, 4031 (2001).

12 H. Brenning, S. Kafanov, T. Duty, S. Kubatkin, and P. Delsing, J. Appl. Phys. **100**, 114321 (2006).

13 A. A. Clerk, S. M. Girvin, A. K. Nguyen, and A. D. Stone, Phys. Rev. Lett. **89**, 176804 (2002).

[14] Yu. Makhlin, G. Schön, and A. Shnirman, Rev. Mod. Phys. **73**, 357 (2001).
[15] P. L. D. Abrie, *Design of RF and Microwave Amplifiers and Oscillators* (Artech House, Boston, 2000).
[16] T. R. Stevenson, F. A. Pellerano, C. M. Stahle, K. Aidala, and R. J. Schoelkopf, Appl. Phys. Lett. **80**, 3012 (2002).
[17] M. Thalakulam, Z. Ji, and A. J. Rimberg, Phys. Rev. Lett. **93**, 066804 (2004).
[18] L. Roschier, P. Hakonen, K. Bladh, P. Delsing, K. W. Lehnert, L. Spietz, and R. J. Schoelkopf, J. Appl. Phys. **95**, 1274 (2004).
[19] A. N. Korotkov and M. A. Paalanen, Appl. Phys. Lett. **74**, 4052 (1999).